Inorganic Chemistry

Article

pubs.acs.org/IC

Dual Luminescent Tetranuclear Organogold(I) Macrocycles of 5,5′-Diethynyl-2,2′-bipyridine and Their Efficient Sensitization of Yb(III) Luminescence

Xiu-Ling Li,*[,†,‡] Ming Tan,[†] Ke-Juan Zhang,[†] Bo Yang,[†] Jie Chen,[†] and Yu-Bo Ai[†]

[†]School of Chemistry and Chemical Engineering and [‡]Jiangsu Key Laboratory of Green Synthetic Chemistry for Functional Materials, Xuzhou Normal University, Xuzhou, Jiangsu 221116, China

Supporting Information

ABSTRACT: Reaction of $(AuC{\equiv}CbpyC{\equiv}CAu)_n$ ($HC{\equiv}CbpyC{\equiv}CH$ = 5,5′-diethynyl-2,2′-bipyridine) with diphosphine ligands $Ph_2P(CH_2)_nPPh_2$ (n = 1 dppm, 3 dppp, 5 dpppen, 6 dpph), 1,1′-bis(diphenylphosphino)ferrocene (dppf), and 1,2-bis(diphenylphosphino)-benzene (bdpp) in CH_2Cl_2 afforded the corresponding dual luminescent gold(I) complexes $[(AuC{\equiv}CbpyC{\equiv}CAu)_2(\mu\text{-dppm})_2]$ (**1**), $[(AuC{\equiv}CbpyC{\equiv}CAu)_2(\mu\text{-dppp})_2]$ (**2**), $[(AuC{\equiv}CbpyC{\equiv}CAu)_2(\mu\text{-dpppen})_2]$ (**3**), $[(AuC{\equiv}CbpyC{\equiv}CAu)_2(\mu\text{-dpph})_2]$ (**4**), $[(AuC{\equiv}CbpyC{\equiv}CAu)_2(\mu\text{-dppf})_2]$ (**5**), and $[(AuC{\equiv}CbpyC{\equiv}CAu)_2(\mu\text{-bdpp})_2]$ (**6**). The solid structures of complexes **1** and **2** are confirmed to be tetranuclear macrocyclic rings by single crystal structure analysis, and those of complexes **3**−**6** are proposed to be similar to those of complexes **1** and **2** in structure because their good solubility in CH_2Cl_2, their HRMS results, and the P···P separations of 20.405−20.697 Å in the same linear rigid P—Au—C≡CbpyC≡C—Au—P unit are all favorable to form such 2:4:2 macrocycles. Each of the absorption spectral titrations between complexes **1**−**6** and $Yb(hfac)_3(H_2O)_2$ (Hhfac = hexafluoroacetylacetone) gives a 2:1 ratio between the $Yb(hfac)_3$ unit and the complex **1**−**6** moieties. The energy transfer occurs efficiently from the gold(I) alkynyl antennas **1**−**6** to Yb(III) centers with the donor ability in the order of **1** ∼ **2** ∼ **3** ∼ **4** > **6** > **5**.

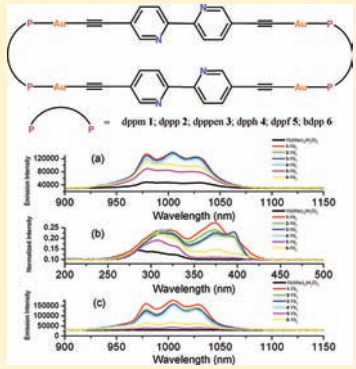

INTRODUCTION

Reaction of gold(I) diacetylides with diphosphine ligands can lead to polymers, 1:2:1 (diacetylide−gold(I)−diphosphine) simple macrocycles, 2:4:2 (diacetylide−gold(I)−diphosphine) macrocycles, and catenanes (see Scheme 1), depending on the geometry and flexibility of the diacetylide ligands and the length of the spacer groups in the diphosphine ligands.[1−13] For compounds $[\{X(4\text{-}C_6H_4OCH_2C{\equiv}CAu)_2(\mu\text{-}Ph_2PZPPh_2)\}_n]$, only in the cases when the hinge group X was a single atom bridge with medium-sized spacer groups Z = $(CH_2)_3$ or $(CH_2)_4$ were [2]catenanes formed.[11] So the judicious choice of hinge group has been a smart strategy for the synthesis of topologically different structures. The secondary bonding effects such as aurophilic attraction, $\pi\cdots\pi$ interaction, and hydrogen bonds are all possible driving forces during catenation.[1−13]

Though a lot of macrocycles have been reported, most of them are about flexible diacetylide ligands with a suitable hinge group;[1−13] those about rigidly linear diacetylide ligands are much reduced in number. The 26-membered $[(AuC{\equiv}CArC{\equiv}CAu)_2(\mu\text{-dcypm})_2]$ (Ar = C_6H_4, $C_6H_2Me_2$) (dcypm is bis(cyclohexylphosphino)methane),[14] 34-membered $[(AuC{\equiv}CC_6H_4{-}C_6H_4C{\equiv}CAu)_2(\mu\text{-dppm})_2]$ and $[(AuC{\equiv}CC_6H_4{-}C_6H_4C{\equiv}CAu)_2(\mu\text{-dcypm})_2]$ (dppm is bis-(diphenylphosphino)methane), and 38-membered $[(AuC{\equiv}CC_6H_4N{=}NC_6H_4C{\equiv}CAu)_2(\mu\text{-dppm})_2]$ are limited examples[10,14,15] in which the CH_2 unit is the spacer group between two phosphorus atoms within each phosphine ligand. It is interesting to explore the use of rigid and longer diacetylide ligands to assemble macrocycle structures. In addition, though all kinds of topological macrocycles for the diacetylide−diphosphine−digold(I) systems have been reported, it is a pity to find that the luminescent properties of most of them were not reported. It was reported that some organometallic Au(I) phosphine acetylides had exhibited phosphorescent properties due to the heavy atom effect of the Au(I) ions or aurophilic interactions.[16−26] In addition, they are stable to air and moisture and can be prepared readily. The intense, long-lifetime phosphorescent ones containing rigid alkyne ligands[16−22,24−26] are in favor of energy transfer in heteronuclear systems.[25,26]

On the other hand, near-infrared (NIR) Ln(III) (Ln = lanthanide) luminescence has been extensively applied to biomedical assays and optical communication and so forth because of its distinct advantages, such as narrow emission bands, long-radiative lifetimes, large Stokes shifts, and relatively immovable emission positions.[25−38] Using the d-block metal-lorganic antenna chromophores with good conjugation as building blocks and sensitizers for Ln(III) luminescence has been proved to be a kind of efficient strategy to overcome the weak absorption from Laporte-forbidden f−f transitions of the

Received: May 31, 2011
Published: December 9, 2011

dx.doi.org/10.1021/ic201741h | Inorg. Chem. 2012, 51, 109−118

Scheme 1. Possible Structures of Diacetylide−Gold(I)−Diphosphine Complexes: (a) Polymer; (b) 1:2:1 Simple Macrocycle; (c) Catenane Consisting of 1:2:1 Simple Macrocycles; (d) 2:4:2 Macrocycle; (e) Catenane Consisting of 2:4:2 Simple Macrocycles

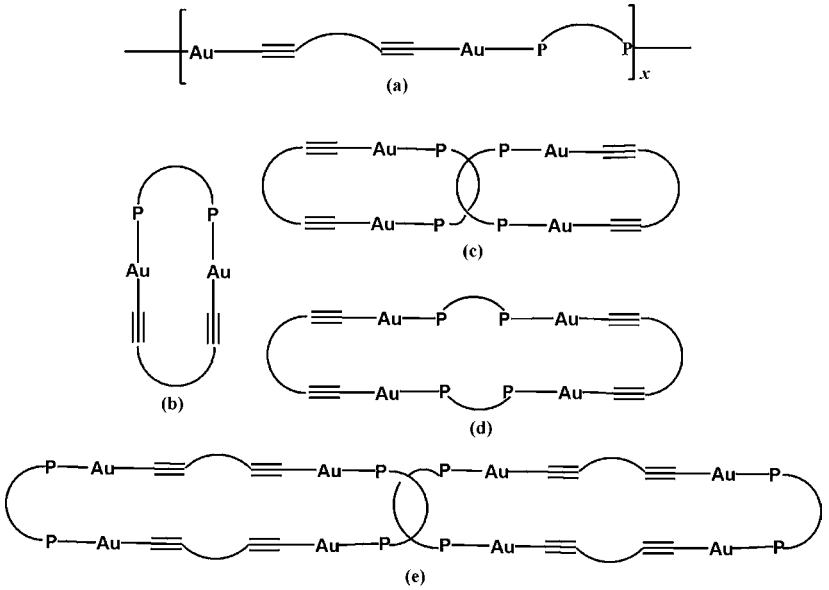

Ln(III) ions.[25−38] Another kind of efficient coordinating unit and the most investigated Ln(III) coordinating units are the β-diketonate ions.[26−32] The two coordinated water molecules in Ln(β-diketonate)$_3$(H$_2$O)$_2$ units can be easily replaced by chelating phenanthroline or polypyridine chromophores, leading to highly luminescent ternary complexes. The polypyridine-functionalized alkynyl ligands have been proved to be good bridging ligands for sensitization of Ln(III) NIR luminescence in our previous work with respect to energy-transfer processes and minimization of nonradiative deactivation in a d−f assembly due to their good chelating abilities, linearity, and conjugacy.[25,27,28] It has been reported by us and others that the Au(I)−phosphine−acetylide chromophores were favorable antenna chromophores for sensitization of lanthanide NIR luminescence when using 4′-(4-ethynylphenyl)-2,2′:6′,2″-terpyridine (tpyC$_6$H$_4$C≡CH) or 5-ethynyl-2,2′-bipyridine (bpyC≡CH) as bridging ligands in the heteronuclear Au(I)−Ln(III) systems.[25,26] But to our best knowledge, using the organogold(I) macrocyclic acetylides as antennas has not been reported so far.

Based on an overall consideration of aforementioned factors, here, 5,5′-diethynyl-2,2′-bipyridine (HC≡CbpyC≡CH) was used to prepare a series of tetranuclear gold(I)−alkynyl−phosphine complexes by depolymerization of polymeric (AuC≡CbpyC≡CAu)$_n$ with diphosphine ligands. Herein, the syntheses, structures, and photophysical properties of these tetranuclear gold(I)−diphosphine−diacetylides and their sensitization of Yb(III) NIR luminescence will be reported.

EXPERIMENTAL SECTION

Materials and Reagents. The reagents dppm, 1,2-bis(diphenylphosphino)ethane (dppe), 1,3-bis(diphenylphosphino)propane (dppp), 1,4-bis(diphenylphosphino)butane (dppb), 1,5-bis(diphenylphosphino)pentane (dpppen), 1,6-bis(diphenylphosphino)hexane (dpph), 1,1′-bis(diphenylphosphino)ferrocene (dppf), 1,2-bis(diphenylphosphino)benzene (bdpp), tetrahydrothiophene (tht), and H[AuCl$_4$]·4H$_2$O were purchased from commercial sources and used as received unless stated otherwise. 5,5′-Bis[2-(trimethylsilyl)-1-ethynyl]-2,2′-bipyridine (SMTC≡CbpyC≡CTMS),[39] HC≡CbpyC≡CH,[39] (AuC≡CbpyC≡CAu)$_n$,[25] and Yb(hfac)$_3$(H$_2$O)$_2$ (Hhfac = hexafluoroacetylacetone) were prepared by the published methods.[40] Diisopropylamine was freshly distilled over CaH$_2$. All solvents were purified and distilled by standard procedures before use, except those for spectroscopic measurements were of spectroscopic grade. All reactions were carried out under a stream of dry argon by using Schlenk techniques at room temperature and a vacuum-line system unless otherwise specified.

Physical Measurements. Infrared (IR) spectra were obtained from KBr pellets using a Bruker Optics TENSOR 27 FT-IR spectrophotometer. UV−vis absorption spectra were recorded on a Purkinje General TU-1901 UV−vis spectrophotometer. Elemental analyses (C, H, N) were carried out on a Perkin-Elmer model 240C elemental analyzer. HRMS analyses were carried out with a Bruker-micro-TOFQ-MS analyzer using a dichloromethane (DCM)/methanol mixture as the mobile phase. Steady-state excitation and emission spectra in the UV−vis region were recorded on a Hitachi F4500 fluorescence spectrophotometer for complexes **1**−**6**. The f−f absorption spectra of Yb(III) centers in the NIR region were carried out on a Shimadzu UV-3150 UV−vis−NIR spectrophotometer. The steady-state Yb(III) NIR emission spectra and their excitation spectra were measured on an Edinburgh FLS920 fluorescence spectrometer equipped with a Hamamatsu R5509-72 supercooled photomultiplier tube at 193 K and a TM300 emission monochromator with a NIR grating blazed at 1000 nm. The NIR emission spectra were corrected via a calibration curve supplied with the instrument. Emission lifetimes were determined on an Edinburgh Analytical Instrument (F900 fluorescence spectrometer) in the air, and the resulting emission was detected with a thermoelectrically cooled Hamamatsu R3809 photomultiplier tube. All the emission and excitation spectra were carried out in the air.

Synthesis. *(AuC≡CbpyC≡CAu)$_n$.* A methanol (5 mL) solution of potassium fluoride (KF) (0.046 g, 0.80 mmol) was added to a solution of Au(tht)Cl (0.256 g, 0.8 mmol) in tetrahydrofuran (THF) (30 mL) in an ice−water bath; then a DCM solution of SMTC≡CbpyC≡CTMS (0.139 g, 0.40 mmol) was dropwise added to the above solution. The mixture was stirred for 3 h; then the orange precipitate of the product was filtered and washed with methanol, THF, DCM, water, and ethanol successively and dried in a vacuum. Yield: 0.215 g, 94%. This product was used without further characterization. ***Caution:*** *Generally speaking, the product (AuC≡CbpyC≡CAu)$_n$, especially the newly prepared product, is safe, but it is*

dx.doi.org/10.1021/ic201741h | Inorg. Chem. 2012, 51, 109−118

shock and scrape sensitive in a very dry state, and it will explode under violent scraping with a stainless steel spoon, so it was kept in a plastic bottle in the refrigerating chamber of the fridge in the absence of light and taken with a plastic spoon or a horn spoon carefully.

*[(AuC≡CbpyC≡CAu)$_2$(μ-dppm)$_2$] (**1**).* Dppm (59.4 mg, 97%, 0.15 mmol) was added to a DCM solution (15 mL) of (AuC≡CbpyC≡CAu)$_n$ (89.4 mg, 0.15 mmol) with stirring at room temperature. After it was stirred for 1 h, the solution was concentrated and the product was purified by chromatography on a very short silica gel column using DCM−methanol (100:2) as eluent. Addition of ethyl ether to the concentrated solution gave the product as a pale yellow powder (yield 126.4 mg, 86%). Anal. Calcd for $C_{78}H_{56}Au_4N_4P_4\cdot1.5CH_2Cl_2$: C, 45.73; H, 2.85; N, 2.68. Found: C, 45.69; H, 2.88; N, 2.64. HRMS (*m*/*z*): 1961.2 [M + H]$^+$, 1561.1 [M − C≡CbpyC≡CAu]$^+$, 981.1 [M − AuCCbpyC≡CAu − dppm + H]$^+$. ^{1}H NMR ($CDCl_3$, ppm): 8.517 (m, 4H, C≡C*bpy*C≡C), 7.828−7.851 (m, 4H, C≡C*bpy*C≡C), 7.579−7.630 (m, 20H, C≡C*bpy*C≡C + P*Ph*$_2$), 7.297−7.414 (m, 24H, P*Ph*$_2$), 5.304 (s, 3H, CH_2Cl_2), 3.729 (m, 4H, PCH_2). IR spectrum (KBr, cm^{-1}): 2111 m (C≡C). Detailed IR data are provided in the Supporting Information.

*[(AuC≡CbpyC≡CAu)$_2$(μ-dppp)$_2$] (**2**).* This compound was prepared by the same synthetic procedure as that of **1** except for using dppp instead of dppm. Color: deep yellow. Yield: 110.4 mg, 73%. Anal. Calcd for $C_{82}H_{64}Au_4N_4P_4$: C, 48.80; H, 3.20; N, 2.78. Found: C, 48.75; H, 3.22; N, 2.73. HRMS (*m*/*z*): 2017.3 [M + H]$^+$, 1617.8 [M − C≡CbpyC≡CAu]$^+$, 1021.3 [Au(dppp)$_2$]$^+$, 1009.1 [M − AuC≡CbpyC≡CAu − dppp + H]$^+$. ^{1}H NMR ($CDCl_3$, ppm): 8.712−8.783 (m, 4H, C≡C*bpy*C≡C), 8.286−8.408 (m, 4H, C≡C*bpy*C≡C), 7.852−7.926 (m, 4H, C≡C*bpy*C≡C), 7.674−7.749 (m, 16H, P*Ph*$_2$), 7.459−7.474 (m, 24H, P*Ph*$_2$), 2.831 (m, 8H, PCH_2), 1.963 (m, 4H, PCH_2CH_2). IR spectrum (KBr, cm^{-1}): 2111 m (C≡C). Detailed IR data are provided in the Supporting Information.

*[(AuC≡CbpyC≡CAu)$_2$(μ-dpppen)$_2$] (**3**).* This compound was prepared by the same synthetic procedure as that of **1** except for using dpppen instead of dppm. Color: pale yellow. Yield: 121.2 mg, 78.0%. Anal. Calcd for $C_{86}H_{72}Au_4N_4P_4$: C, 49.80; H, 3.50; N, 2.70. Found: C, 49.73; H, 3.46; N, 2.65. HRMS (*m*/*z*): 2073.4 [M + H]$^+$, 1037.2 [M − AuC≡CbpyC≡CAu − dpppen + H]$^+$. ^{1}H NMR ($CDCl_3$, ppm): 8.790 (m, 4H, C≡C*bpy*C≡C), 8.281−8.392 (m, 4H, C≡C*bpy*C≡C), 7.855−7.912 (m, 4H, C≡C*bpy*C≡C), 7.652−7.732 (m, 16H, P*Ph*$_2$), 7.501 (sbr, 24H, P*Ph*$_2$), 2.415 (m, 8H, PCH_2), 1.690 (sbr, 12H, P$CH_2CH_2CH_2$). IR spectrum (KBr, cm^{-1}): 2107 m (C≡C). Detailed IR data are provided in the Supporting Information.

*[(AuC≡CbpyC≡CAu)$_2$(μ-dpph)$_2$] (**4**).* This compound was prepared by the same synthetic procedure as that of **1** except for using dpph instead of dppm. Color: pale yellow. Yield: 117.8 mg, 74.8%. Anal. Calcd for $C_{88}H_{76}Au_4N_4P_4$: C, 50.28; H, 3.65; N, 2.67. Found: C, 50.36; H, 3.59; N, 2.65. HRMS (*m*/*z*): 2101.4 [M + H]$^+$, 1051.2 [M − AuC≡CbpyC≡CAu − dpph + H]$^+$. ^{1}H NMR ($CDCl_3$, ppm): (m, 4H, C≡C*bpy*C≡C), 8.384−8.410 (m, 4H, C≡C*bpy*C≡C), 7.857−7.943 (m, 4H, C≡C*bpy*C≡C), 7.626−7.678 (m, 16H, P*Ph*$_2$), 7.472−7.521 (m, 24H, P*Ph*$_2$), 2.396 (m, 8H, PCH_2), 1.592 (m, 8H, PCH_2CH_2), 1.475 (m, 8H, P$CH_2CH_2CH_2$). IR spectrum (KBr, cm^{-1}): 2110 m (C≡C). Detailed IR data are provided in the Supporting Information.

*[(AuC≡CbpyC≡CAu)$_2$(μ-dppf)$_2$] (**5**).* This compound was prepared by the same synthetic procedure as that of **1** except for using dppf instead of dppm. Color: pale yellow. Yield: 118.0 mg, 68.4%. Anal. Calcd for $C_{96}H_{68}Au_4Fe_2N_4P_4$: C, 50.08; H, 2.98; N, 2.44. Found: C, 49.95; H, 2.93; N, 2.40. HRMS (*m*/*z*): 2301.2 [M + H]$^+$, 1901.2 [M − C≡CbpyC≡CAu]$^+$, 1705.2 [M − AuC≡CbpyC≡CAu + H]$^+$, 1151.1 [M − AuC≡CbpyC≡CAu − dppf + H]$^+$. ^{1}H NMR ($CDCl_3$, ppm): 8.821−8.777 (m, 4H, C≡C*bpy*C≡C), 8.306−8.431 (m, 4H, C≡C*bpy*C≡C), 7.892−7.916 (m, 4H, C≡C*bpy*C≡C), 7.456−7.596 (m, 40H, P*Ph*$_2$), 4.765 (m, 8H, $C_{10}H_8$Fe), 4.313 (m, 8H, $C_{10}H_8$Fe). IR spectrum (KBr, cm^{-1}): 2111 m (C≡C). Detailed IR data are provided in the Supporting Information.

*[(AuC≡CbpyC≡CAu)$_2$(μ-bdpp)$_2$] (**6**).* This compound was prepared by the same synthetic procedure as that of **1** except for using bdpp instead of dppm. Color: yellow. Yield: 87.1 mg, 55.7%. Anal. Calcd for $C_{88}H_{60}Au_4N_4P_4$: C, 50.67; H, 2.90; N, 2.69. Found: C, 50.73; H, 2.91; N, 2.75. HRMS (*m*/*z*): 2085.3 [M + H]$^+$, 1089.3 [Au(bdpp)$_2$]$^+$, 1043.1 [M − AuC≡CbpyC≡CAu − bdpp + H]$^+$. IR spectrum (KBr, cm^{-1}): 2099 m (C≡C). Detailed IR data are provided in the Supporting Information.

Crystal Structure Determination. Crystals suitable for X-ray diffraction studies for **1**·3CH_2Cl_2 and **2**·2C_6H_7N·C_6H_6·2CH_2Cl_2·2H_2O were obtained by layering *n*-hexane onto the corresponding DCM or the DCM/aniline/benzene solution in the absence of light. Single crystals were sealed in capillaries with mother liquors. Complexes **1**·3CH_2Cl_2 and **2**·2C_6H_7N·C_6H_6·2CH_2Cl_2·2H_2O were measured on the RIGAKU SCXmini and RIGAKU MERCURY CCD diffractometers, respectively, by the ω scan technique at room temperature with graphite-monochromated Mo Kα radiation (λ = 0.71073 Å). The CrystalClear software packages[41,42] and Bruker SAINT were used for data reduction and empirical absorption correction,[43] respectively. The structures were solved by direct methods. The heavy atoms were located from E-map, and the rest of the non-hydrogen atoms were found in subsequent Fourier maps. The non-hydrogen atoms were refined anisotropically, whereas the hydrogen atoms were generated geometrically with isotropic thermal parameters. The structures were refined on F^2 by full-matrix least-squares methods using the SHELXTL-97 program package.[44] The crystallographic data of **1**·3CH_2Cl_2 and **2**·2C_6H_7N·C_6H_6·2CH_2Cl_2·2H_2O are summarized in Table 1.

Table 1. Crystallographic Data for 1·3CH_2Cl_2 and 2·2C_6H_7N·C_6H_6·2CH_2Cl_2·2H_2O

	1·3CH_2Cl_2	**2**·2C_6H_7N·C_6H_6·2CH_2Cl_2·2H_2O
formula	$C_{81}H_{62}Au_4Cl_6N_4P_4$	$C_{102}H_{92}Au_4Cl_4N_6O_2P_4$
fw	2215.79	2487.36
temp, K	293(2)	293(2)
space group	$P\bar{1}$	$C2/c$
a, Å	16.9861(15)	23.013(5)
b, Å	17.2304(17)	22.507(5)
c, Å	22.451(3)	21.968(4)
α, deg	78.7730(10)	
β, deg	81.930(2)	117.79(3)
γ, deg	75.3510(10)	
V, Å^3	6206.7(11)	10066(3)
Z	3	4
ρ_{calcd}, mg·m^{-3}	1.778	1.641
μ, mm^{-1}	7.383	6.031
radiation (λ, Å)	0.71073	0.71073
R1[a]	0.0960	0.0785
wR2[b]	0.1989	0.1720
GOF	0.965	1.095

[a] $R1 = \sum|F_o - F_c|/\sum F_o$. [b] $wR2 = \sum[w(F_o^2 - F_c^2)^2]/\sum[w(F_o^2)]^{1/2}$.

RESULTS AND DISCUSSION

Syntheses of Tetranuclear Gold(I) Complexes and Characterization. The reaction of [(AuCl)$_2$(μ-dcypm)] or [(AuCl)$_2$(μ-dppm)] with the corresponding rigid diacetylide in the presence of base has been used to assemble the similar tetranuclear gold(I) ring by Puddephatt's group and Yam's group,[14,15] while complexes **1**−**6** were prepared by general methods established previously[25] through the reaction of the corresponding diphosphine ligands with 1 equiv of digold(I) diacetylides (AuC≡CbpyC≡CAu)$_n$ (see Scheme 2) and purified by chromatography on very short silica gel columns using DCM−methanol (100:2) as eluent. Complexes **1**−**6** were isolated as air-stable pale yellow to deep yellow solids. Subsequent recrystallization was carried out by slow diffusion

dx.doi.org/10.1021/ic201741h | *Inorg. Chem.* 2012, 51, 109−118

Scheme 2. Synthetic Routes to Complexes 1−6

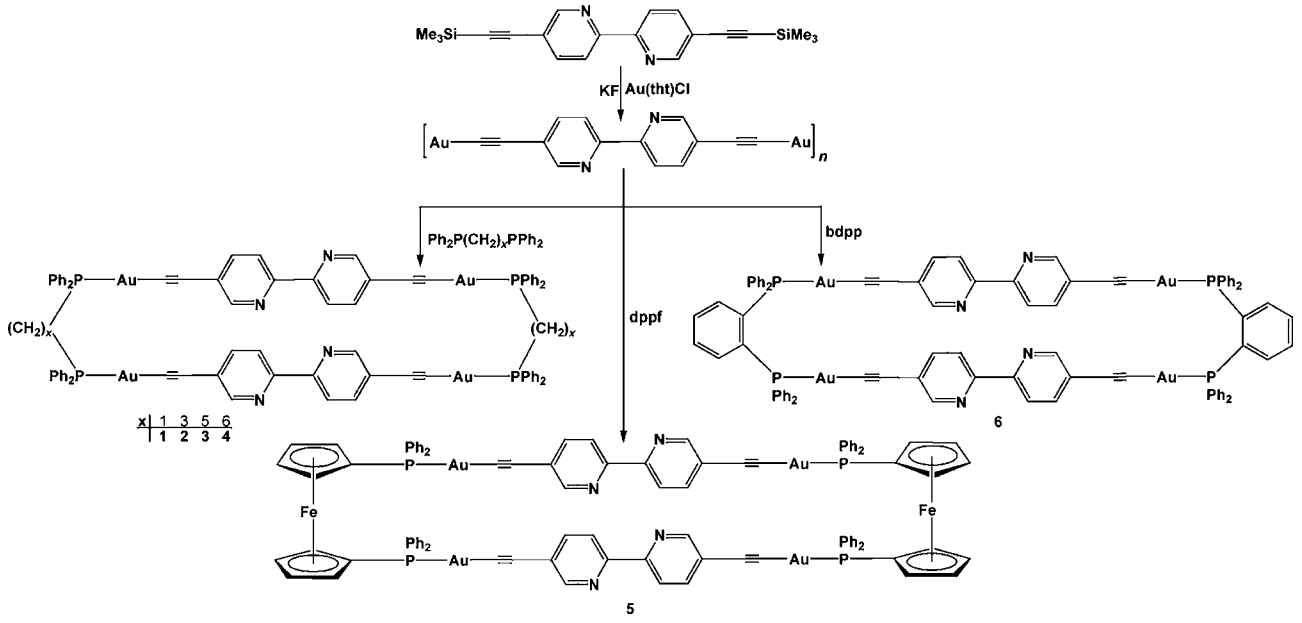

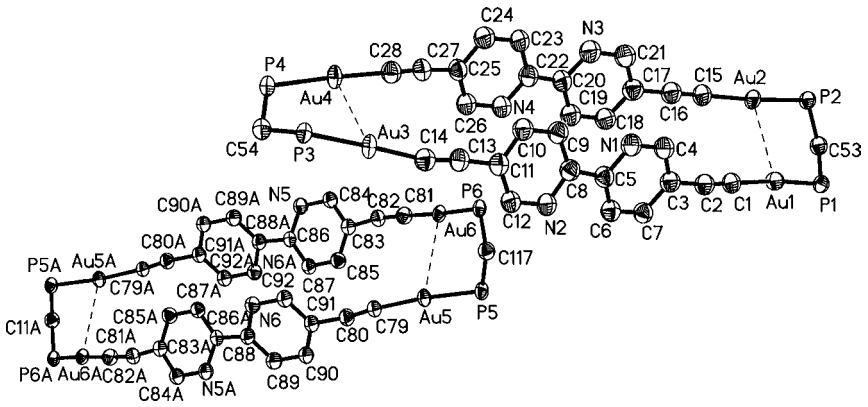

Figure 1. Perspective drawing of **1**·3CH_2Cl_2 with atom labeling scheme. Thermal ellipsoids are shown at the 30% probability level. Phenyl rings of dppm, CH_2Cl_2 molecules, and hydrogen atoms are omitted for clarity. (Symmetry code for A: $-x$, $-y$, $-z + 2$).

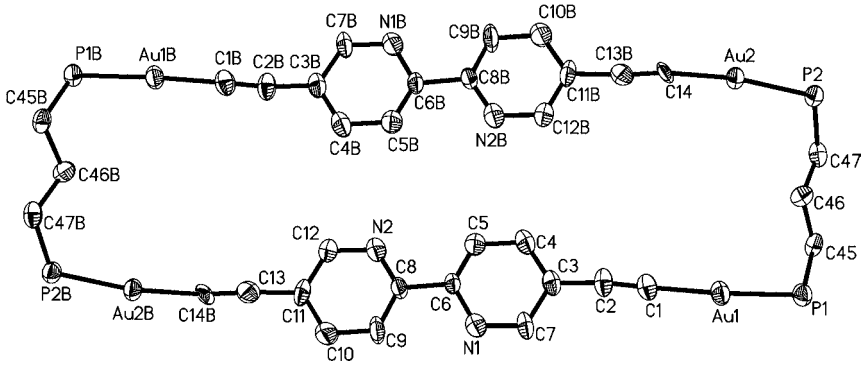

Figure 2. Perspective drawing of a macrocycle of complex **2** with atom labeling scheme. Thermal ellipsoids are shown at the 30% probability level. Phenyl rings of dppp, solvent molecules, and hydrogen atoms are omitted for clarity. (Symmetry code for B: 1.5 − x, 1.5 − y, 1.0 − z.)

of *n*-hexane into the corresponding concentrated DCM solutions, and pale yellow crystals of complex **1** were obtained by this method. Many attempts were made to grow crystals of complexes **2**−**6**, but finally only orange crystals of complex **2** were obtained by layering *n*-hexane onto the solution of mixed solvents of DCM, aniline, and benzene in the absence of light.

All the complexes **1**−**6** are air-stable solids, which are soluble in organic solvents such as DCM solution and chloroform. All the complexes **1**−**6** have been characterized by IR spectroscopy, positive HRMS mass spectroscopy, and elemental analysis. The ^{1}H NMR spectroscopy of complexes **1**−**5** was also studied. Complex **6** was not characterized by its ^{1}H NMR spectrum

dx.doi.org/10.1021/ic201741h | *Inorg. Chem.* 2012, 51, 109−118

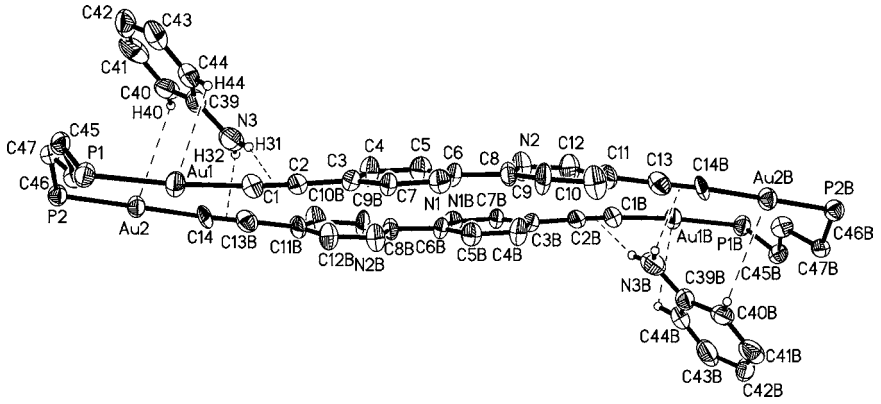

Figure 3. Weak interactions between aniline molecules and the macrocycle of complex **2**. Phenyl rings of dppp, and most hydrogen atoms are omitted for clarity. (Symmetry code for B: 1.5 − *x*, 1.5 − *y*, 1.0 − *z*.)

because all the hydrogen atoms are about phenyl and bpy groups. All the tetranuclear gold(I)−phosphine−acetylide complexes exhibit ν(C≡C) stretching modes from 2099 cm^{-1} to 2111 cm^{-1}, which fall into the usual range for terminal σ-coordinated alkynyl ligands.[25−28] No lower frequency for the ν(C≡C) bands was observed, indicating no π-coordination mode of the C≡C bond exists.

Crystallographic Studies. The crystal structures of complexes **1**·3CH_2Cl_2 and **2**·2C_6H_7N·C_6H_6·2CH_2Cl_2·2H_2O have been determined and confirmed by single crystal X-ray diffraction. They crystallized in the triclinic system with space group $P\bar{1}$ and in the monoclinic system with space group $C2/c$, respectively. Selected bond lengths and bond angles are presented in Table S1 (see the Supporting Information).

Complexes **1** and **2** are formed by [2 + 2] self-assembly of the digold(I) diacetylide and diphosphine components into 34-membered and 38-membered 2:4:2 (diacetylide−gold(I)−diphosphine) macrocycles, respectively (see Figures 1 and 2). The Au(I) centers in both complexes adopt quasilinear coordination geometries, as reported in many gold(I)−acetylide−phosphine complexes,[1−26] and the C−Au−P angles are in the range 171.4(4)−176.9(10)°, which shows some deviation from 180° slightly. The bond distances of Au−P (2.265(7)−2.285(6) Å) and Au−C (1.95(3)−2.06(3) Å) are in good agreement with the lengths reported in Au−acetylide systems.[1−26] The C≡C distances (1.16(4)−1.25(4) Å) are comparable to those in the similar dinuclear gold(I)−arylacetylide−phosphine complexes.[25]

The unit cell of complex **1**·3CH_2Cl_2 consists of three 2:4:2 rings of complex **1** and nine DCM solvent molecules.[3,5,11] The bridging dppm adopts a *cis*-conformation, with the angles Au1−P1···Au2−P2 = 12.7°, Au3−P3···Au4−P4 = 19.7°, and Au5−P5···Au6−P6 = 27.9°, as in other gold(I) complexes with bridging *cis*-dppm ligands.[4,10,45−47] The two Au···Au units in the macrocycle with boat conformation containing Au1, Au2, Au3, and Au4 are twisted against each other with a separation angle of 24.7°, while the dihedral angle between the two dialkyne ligands is 8.8°; it can therefore avoid the larger repulsion resulting from face-to-face arrangement. The second macrocycle with chair conformation containing Au5 and Au6 is centrosymmetric, but two dialkyne parts in the asymmetrical units still adopt the offset face-to-face mode, with a dihedral angle of 28.4° to avoid being parallel to each other. The dihedral angle between the plane of Au1, Au2, Au3, and Au4 and that of Au5, Au5A, Au6, and Au6A is 122.8°.

The 34-membered macrocycles of complex **1** are further stabilized by the intramolecular aurophilic attractions with 3.096(2) Å for Au1···Au2, 3.266(2) Å for Au3···Au4, and 3.258(2) Å for Au5···Au6 (see Table S1 of the Supporting Information and Figure 1),[8,25] while the closest intermolecular Au···Au distances are 5.938 Å, which are much larger than 3.6 Å, indicating the absence of intermolecular Au···Au interaction.[19,25] The nonbonded P···P distance within each dppm is 3.063, 3.037, and 3.022 Å for P1···P2, P3···P4, and P5···P6, respectively, and such short distances support the weak intramolecular Au···Au interactions. The lack of intermolecular Au···Au interactions is probably due to the steric hindrance exerted by the neighboring dppm ligands, which prevents the close approach of the molecules.

The original purpose of adding aniline into the mixed solvents was to expect that intermolecular hydrogen bonds could be formed between aniline and the macrocycles to promote the crystallization of complex **2**−**6**, and thereby good crystals suitable for single crystal X-ray diffraction could be obtained. It is a pleasant surprise to see such an expectation comes true finally in complex **2**·2C_6H_7N·C_6H_6·2CH_2Cl_2·2H_2O. Complex **2** crystallizes with some solvents, including two aniline molecules, one benzene molecule, two DCM molecules, and two water molecules. The centrosymmetric 38-membered macrocycle with chair conformation of complex **2** is constructed from two AuC≡CbpyC≡CAu units and two dppp spacers (see Figure 2), similar to that macrocycle of complex **1**, but showing a little difference. The nonbonded P···P distance within each dppp in complex **2** is 5.529 Å, a distance which is large enough to disfavor the formation of intramolecular Au···Au interactions between the linear rigid P−Au−C≡CbpyC≡C−Au−P units. In fact, the distance between Au1 and Au2 is 5.963 Å, much larger than 3.6 Å, confirming the absence of intramolecular Au···Au interactions.[19,25] As shown in Figure 3, two aniline molecules catch hold of the ring of complex **2** through N−H···π hydrogen bonds between the $-NH_2$ group and the C≡C units ($d_{H31\cdots X1}$ = 2.673 Å, $d_{N3\cdots X1}$ = 3.380 Å, ∠N3−H31···X1 = 161.1°, and $d_{H32\cdots X2}$ = 2.555 Å, $d_{N3\cdots X2}$ = 3.493 Å, ∠N3−H32···X2 = 159.7°; X1 and X2 denote the centers of C1 and C2, and C13B (B: 1.5 − *x*, 1.5 − *y*, 1.0 − *z*) and C14, respectively). Though the nitrogen atom of the amine group sometimes could coordinate to the Au(I) center in the gold(I) acetylides,[48,49] its donating ability as a soft donor is much poorer than that of the phosphorus atom for the soft acceptor gold(I).

dx.doi.org/10.1021/ic201741h | *Inorg. Chem.* 2012, 51, 109−118

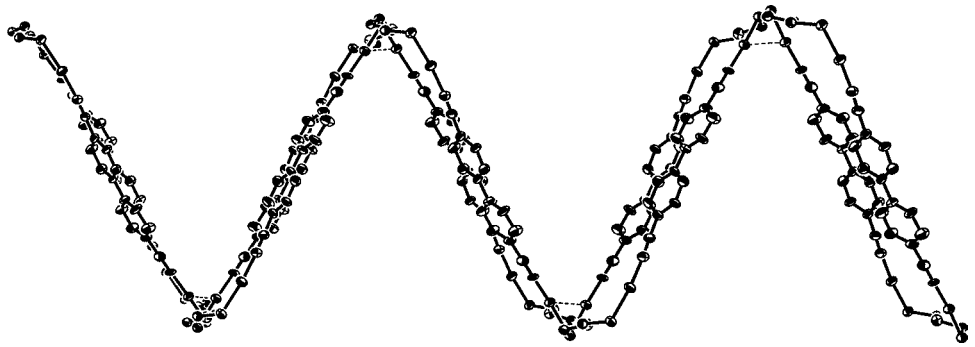

Figure 4. 1-D zigzag chain of complex **2** resulting from intermolecular Au···Au interactions along the *a*-axis. Phenyl rings of dppp and hydrogen atoms are omitted for clarity.

The C−H···Au interactions between the phenyl ring of aniline molecules and the gold(I) centers further strengthen the interactions between aniline and the macrocycle of complex **2** ($d_{H44\cdots Au1}$ = 3.065 Å, ∠C44−H44···Au1 = 123.1°, $d_{H40\cdots Au2}$ = 3.066 Å, ∠C40−H40···Au2 = 120.1°). It should be mentioned that although the C−H···Au angles here are less than 130°, the C−H···Au interactions between aniline molecules and gold(I) centers are suggested to be considered because of their synergistic effects with N−H···π hydrogen bonds in strengthening the interactions between aniline molecules and the macrocycle. The two aniline molecules, like two butterflies, grasp the macrocycle of complex **2**. By contrast to the large intramolecular Au···Au distances, the intermolecular Au2···Au2C (C: 1.5 − *x*, *y*, 0.5 − *z*) distance is only 3.177 Å, indicating the presence of an intermolecular Au···Au interaction, leading to a 1-D ziazag chain structure of macrocycles (see Figure 4).

All the bipyridine groups adopt the expected *trans* configuration to minimize the steric congestion between aromatic protons in complexes **1** and **2**.

Though crystals of complexes **3**−**6** suitable for single crystal X-ray analysis were not obtained, it is speculated that complexes **1**−**6** have similar 2:4:2 macrocyclic structures (ring sizes for **3**, 42; **4**, 44; **5**, 38; **6**, 36). Such speculation is based on the following aspects. First of all, all the compounds have been purified by chromatography on silica gel columns using DCM−methanol (100:2) as eluent. The ionic products in this system impossibly come down with DCM−methanol (100:2) as eluent. In fact, the products with dark color were found to remain at the upper layer of the silica gel columns, so all the products from the silica gel columns are suggested to have neutral frameworks—polymers or rings. Second, they display good solubility in DCM, ruling out the polymeric structures as shown in Scheme 1a and suggesting macrocyclic structures.[50] Third, the largest P···P distance within each dpph molecule in the reported complexes containg Au_2(dpph) units in CCDC is smaller than 10 Å, much smaller than the distances 20.405−20.697 Å of the corresponding P···P separation of each P—Au—C≡CbpyC≡C—Au—P unit in complexes **1** and **2**, to say nothing of those in other diphosphine ligands: dpppen, dppf, dppp, bdpp, and dppm, which have decreasing sizes of P···P separations. So structures containing simple 1:2:1 macrocycles as shown in Scheme 1b and c are not possible for complexes **1**−**6** because of the small P···P distances, although a lot of simple 1:2:1 macrocycles have been reported for the flexible dialkyne ligands.[1,5,7,8,11,12] Even though, in some cases, such 1:2:1 macrocycles can be formed, the ring strain would be too great. Fourth, the HRMS results also support their 2:4:2 macrocyclic structures.[3,51,52] The expected peaks [M + H]$^+$ of parent ions at 1961.2, 2017.3, 2073.4, 2101.4, 2301.2, and 2085.3 corresponding to 2:4:2 macrocycles have been found for complexes **1**−**6**. Finally, though the longest fore-and-aft distance in the macrocycle of complex **2** is 21.895 Å for C47···C47A, the lateral intramolecular Au1···Au2 distance is only 5.963 Å, so the cavity of the macrocycle is not large enough to allow catenation, to say nothing of complex **1**. Furthermore, in complexes **1**−**6**, no hinge group exists in the linear rigid C≡CbpyC≡C unit, and the dihedral angles between two pyridine groups in each P—Au—C≡CbpyC≡C—Au—P unit are 5.6 − 12.2° in complex **1** and 4.7° in complex **2**, which does not favor the catenation.[4,11] Hence, it can also rule out the catenane structures as shown in Scheme 1e induced by the self-assembly of such 2:4:2 macrocycles for complexes **1**−**6**. To explore on a deep level, it is suggested that the 2:4:2 macrocyclic structure of complex **6** is more similar to that of complex **1** instead of complex **2** because the small P···P separation within each bdpp ligand favors the intramolecular Au···Au interaction, and a similar macrocyclic structure has been reported in the cation $[Au_4(bdpp)_2(bipyen)_2]^{4+}$, which contained relatively rigid bipyen ligands (bipyen =1,2-*trans*-bis(4-pyridyl)ethylene).[53] The intramolecular Au···Au distance in this cation was 2.982(1) Å, indicating a strong aurophilic interaction.[53] While the 2:4:2 macrocyclic structures of complexes **3**−**5** are suggested to be more similar to that of complex **2** because the larger P···P separations disfavor intramolecular Au···Au interaction.

To the best of our knowledge, the largest 2:4:2 macrocycle for gold(I)−diphosphine-flexible dialkyne ligands occurred in the doubly braided [2]catenation $[\{[\mu\text{-}X(4\text{-}C_6H_4OCH_2C{\equiv}CAu)_2][\mu\text{-}(Ph_2PCH_2CH_2CH_2CH_2PPh_2)]\}_n]$ (X = cyclohexylidene and *n* = 4), which contained two interlocked 50-membered 2:4:2 $[\{[\mu\text{-}X(4\text{-}C_6H_4OCH_2C{\equiv}CAu)_2][\mu\text{-}(Ph_2PCH_2CH_2CH_2CH_2PPh_2)]\}_2]$ rings,[3] but for rigid dialkyne ligands, the largest reported 2:4:2 ring was 38-membered $[(AuC{\equiv}CC_6H_4N{=}NC_6H_4C{\equiv}CAu)_2(\mu\text{-dppm})_2]$,[15] so here the speculated 44-membered macrocycle of complex **4** may be the largest 2:4:2 macrocycle reported in gold(I)−diphosphine−rigid dialkyne systems. On the other hand, when the diphosphine ligands dppe and dppb were used to try to synthesize the similar 2:4:2 macrocyclic complexes, it was not found to be successful, because insoluble complexes were found to be formed. The insolubility of the products suggested, but not proved, the diphosphine ligands dppe and dppb adopted a *trans* conformation and the zigzag polymers were the dominant products. Therefore, they were not further studied and discussed here.

dx.doi.org/10.1021/ic201741h | *Inorg. Chem.* 2012, 51, 109−118

Photophysical Properties. *Absorption Spectra.* UV−vis absorption data of **1**−**6** in DCM solutions at room temperature are summarized in Table 2. The corresponding

Table 2. Photophysical Data of Complexes 1−6 at 298 K

compd	λ_{abs}/nm	λ_{em}/nm (solid)	λ_{em}/nm (CH_2Cl_2)
HC≡CbpyC≡CH	268, 313, 327		
1	230, 343, 368	468, 555	398, 549, 589
2	233, 339, 357	463, 549	392, 534(w), 573
3	232, 340, 358	455, 551	391, 532, 572
4	232, 340, 358	456, 544	392, 531, 572
5	229, 342, 358	467, 530	393
6	230, 346, 368	468, 556	402, 542, 586

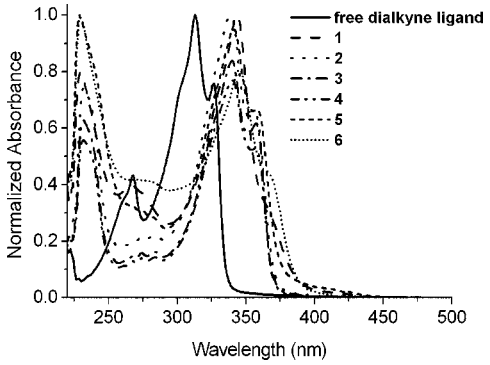

Figure 5. UV−vis absorption spectra of complexes **1**−**6** in DCM solutions at 298 K.

electronic absorption spectra are depicted in Figure 5. Though the spacers between two P donors in the diphosphine ligands change, the absorption spectra of complexes **1**−**6** are very similar throughout the series, and they all display two distinct absorption bands with one maximum at ca. 230 nm and the other at ca. 340 nm with a shoulder absorption at ca. 358 nm for complexes **2**−**5** and 368 nm for complexes **1** and **6** with the tails extending to ca. 450 nm. By comparison with the corresponding absorptions of free HC≡CbpyC≡CH ligands, the former higher-energy bands are assigned to diphosphine-centered transitions,[25] while the latter lower-energy bands are very similar to those of free HC≡CbpyC≡CH ligand and complex Ph_3P—Au—C≡CbpyC≡C—Au—PPh_3 containing the same dialkyne ligand in shape,[22] so they are proposed to be dominated by intraligand $\pi \rightarrow \pi^*$ transitions of the C≡CbpyC≡C units. Such assignment is confirmed by DFT calculations.[22] The vibronic spacings of low-energy absorption bands for complexes **2**−**5** are in the range 1306−1487 cm^{-1}, while those for complexes **1** and **6** are 1980 cm^{-1} and 1727 cm^{-1}, respectively, corresponding to vibrational stretching frequencies of the pyridyl and C≡C units of the C≡CbpyC≡C ligand, respectively, further supporting such an assignment. The obviously red-shifted character with ca. 27−37 nm of complexes **1**−**6** compared to those of free HC≡CbpyC≡CH ligand and the similarity in shape with free HC≡CbpyC≡CH ligand indicates that the formation of tetranuclear macrocycles does not significantly influence the transition character of the singlet state, but it enlarges the conjugation degrees and reduces the π−π^* energy level. It is worthy of note that the low-energy bands of complexes **1** and **6** are much more similar to each other with similar absorption maxima and larger red-shifts than those of complexes **2**−**5**, suggesting that there perhaps are Au···Au interactions for complexes **1** and **6** in DCM solutions.

Absorption Spectra Titration. It is very obvious that the bipyridine units are still free of coordination in complexes **1**−**6**, as seen and concluded from the above structures; hence, these tetranuclear gold(I)−alkynyl−phosphine complexes can be expected to be building blocks through the bipyridine chelating to combine Ln(III) ions to form Au(I)−Ln(III) heteronuclear complexes as reported in our previous work.[25,27,28] In order to explore how the spectra change when Au(I)−Ln(III) heteronuclear complexes form, UV−vis absorption titrations between the DCM solutions of complexes **1**−**6** and the DCM solution of $Yb(hfac)_3(H_2O)_2$ were carried out. Figure 6a and

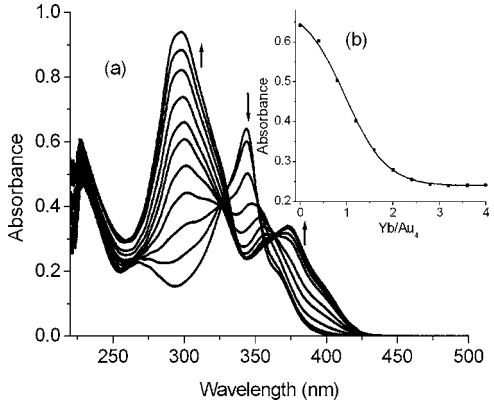

Figure 6. (a) Changes in the UV−vis absorption spectra by titration of **1** with $Yb(hfac)_3(H_2O)_2$ in DCM. (b) Changes of absorbance at 344 nm versus the ratio of the Yb to Au_4 moieties by titration of **1** with $Yb(hfac)_3(H_2O)_2$ in DCM.

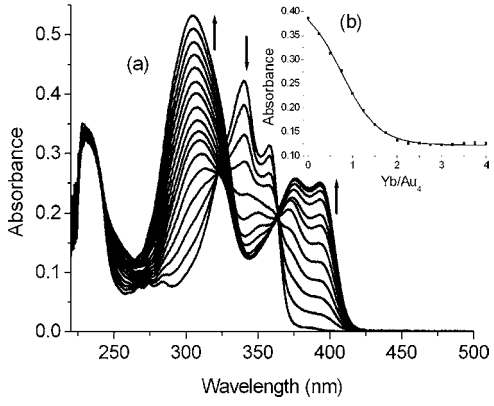

Figure 7. (a) Changes in the UV−vis absorption spectra by titration of **4** with $Yb(hfac)_3(H_2O)_2$ in DCM. (b) Changes of absorbance at 344 nm versus the ratio of the Yb to Au_4 moieties by titration of **4** with $Yb(hfac)_3(H_2O)_2$ in DCM.

Figure 7a show how the absorption spectra change little by little following the addition of the DCM solution of $Yb(hfac)_3(H_2O)_2$ to those of **1** and **4** gradually. The graphs of absorbance at 344 nm give smooth curves that fit well to the 2:1 binding ratios of Yb/Au_4 (see Figure 6b and Figure 7b). The absorption spectra titrations between complexes **2**, **3**, **5**, **6**,

dx.doi.org/10.1021/ic201741h | *Inorg. Chem.* 2012, 51, 109−118

and $Yb(hfac)_3(H_2O)_2$ are provided in Figures S1 to S4 (see Supporting Information), and similar conclusions can be obtained. Compared to those of complexes **1**−**6**, the Au(I) alkynyl based low energy bands are reduced in absorbance and shifted to a more visible region from the maxima at ca. 340 nm to ca. 370 nm, indicating that the conjugation degree is further enlarged and the $\pi-\pi^*$ energy level is also further lowered as a consequence of the formation of Au(I)−Ln(III) heteronuclear complexes.[25−28] An analogous situation has been observed and discussed for $PtLn_2$, Pt_2Ln_4, Au_2Ln_2, and Au_4Ln_4 systems.[25−28]

Luminescence. The luminescent data of **1**−**6** are presented in Table 2. As shown in Figures 8 and 9, both

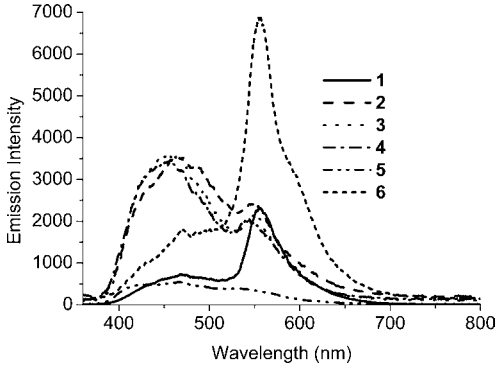

Figure 8. Emission spectra of complexes **1**−**6** in the solid state at room temperature.

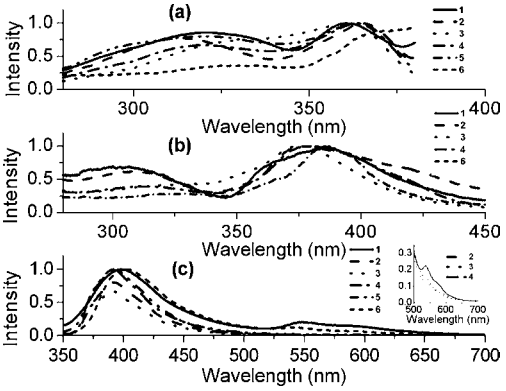

Figure 9. Excitation and emission spectra for complexes **1**−**6** in DCM solutions in the air at room temperature. (a) Excitation spectra with the high energy emission λ_{em} = 391−402 nm. (b) Excitation spectra with the low energy emission λ_{em} = 530−549 nm. (c) Emission spectra upon excitation at λ_{ex} = 330 nm. (top right corner: The amplified emission spectra of complexes **2**−**4** from 500 to 700 nm.)

complexes **1**−**6** in the solid state and complexes **1**, **2**, **3**, **4**, and **6** in DCM solution exhibit dual emission at room temperature. Complexes **1**, **2**, **3**, **4**, and **6** show similar emission bands in shape and positions, but the low energy band of complex **5** was not observed in DCM solution. On the basis of the same reason discussed above in the structure and absorption spectra, the emission bands of complexes **2**−**4** are more similar to one another, and those of complexes **1** and **6** also show greater similarity to each other than to those of complexes **2**−**4**. The low-energy bands for complexes **1**, **2**, **3**, **4**, and **6** in the DCM solutions display vibronic character with spacings in the range 1237−1385 cm^{-1}, which are typical of the ν(C≡C) and ν(C≡N) aromatic vibrational modes in the alkynyl ligands.[25,27,28] Compared with the emission spectrum of HC≡CbpyC≡CH and those of the reported gold(I)−alkynyl−phosphine complexes together with considering the Stokes' shifts,[22,25,26] the high-energy emission bands of complexes **1**−**6** in the range 455−468 nm in the solid state and 391−402 nm in DCM solutions are primarily attributed to the $^1(\pi\rightarrow\pi^*)$ excited state of the C≡CbpyC≡C unit, while the low-energy emission bands at ca. 530−556 nm in the solid state and 531−549 nm in DCM solutions are mainly assigned to the $^3(\pi\rightarrow\pi^*)$ excited state of the acetylide ligand, probably mixed with some ^{3}MMLCT character for complexes **1** and **6** due to the possible intramolecular Au···Au interactions. As shown in Figure 9a and b, in DCM solutions, the maximum excitation wavelengths of the high energy emission bands fall in the range 361−371 nm, which are very close to those maximum absorption wavelengths of intraligand $\pi\rightarrow\pi^*$ transitions of the C≡CbpyC≡C units in complexes **1**−**6**, while those of low energy bands fall in the range 375−387 nm, which are corresponding to the extending region of intraligand $\pi\rightarrow\pi^*$ transitions of the C≡CbpyC≡C units. When oxygen is removed by bubbling argon, the emission intensities of the low energy emission in DCM solutions of complexes **1**−**4** and **6** are dramatically increased compared to those of the corresponding aerated solutions, further demonstrating the triplet state character of the low energy emission.[54] No obvious triplet state emission was observed for complex **5** in DCM solution, and probably the potentially phosphorescence is quenched by an intramolecular energy transfer to the ferrocene units.[54]

Sensitized Yb(III) Luminescence. The following **1**−Yb_2 to **6**−Yb_2 solutions were prepared from complexes **1** to **6** and $Yb(hfac)_3(H_2O)_2$ according to the corresponding ratio 1:2 with the same concentration of $Yb(hfac)_3$ units at 4.432 × 10^{-6} mol·L^{-1}. The symbols **1**−Yb_2 to **6**−Yb_2 here only represent the 2:1 binding ratios of Yb/Au_4 and are used to study the sensitized Yb(III) emission. These symbols have nothing to do with the detailed structures, because whether the tetranuclear gold cores can be still kept when Au(I)−Ln(III) hetronuclear complexes form is not known. As shown in Figure 10a, upon

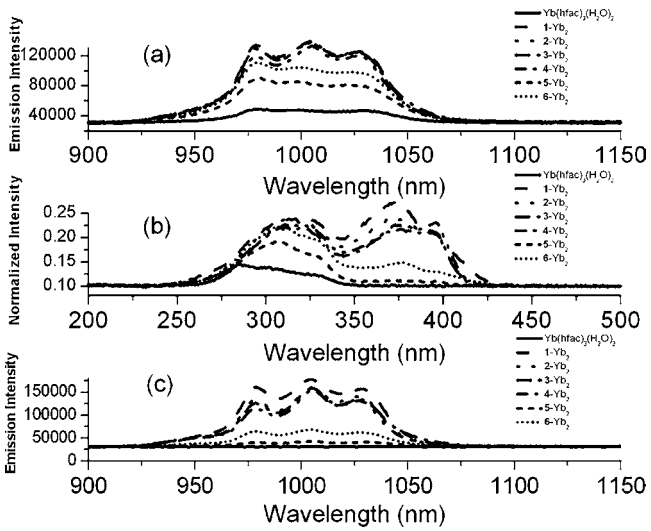

Figure 10. Yb(III) centered excitation and emission spectra of $Yb(hfac)_3(H_2O)_2$ and **1**−Yb_2 to **6**−Yb_2 DCM solutions at 298 K. (a) Emission spectra upon excitation at 310 nm; (b) excitation spectra with the emissions at 979 nm; (c) Yb(III) centered emission spectra upon excitation at 375 nm.

dx.doi.org/10.1021/ic201741h | Inorg. Chem. 2012, 51, 109−118

excitation with λ_{ex} = 310 nm, the **1**−Yb_2 to **6**−Yb_2 DCM solutions display obvious enhancement in intensity of the Yb(III) centered emission relative to that of the Yb(hfac)$_3$(H_2O)$_2$ DCM solution. Their emission intensities at ca. 979 nm are 2.80, 2.80, 2.85, 2.72, 1.85, and 2.27 times of that of Yb(hfac)$_3$(H_2O)$_2$ DCM solution, respectively. Furthermore, as shown in the excitation spectra of the Yb(III) centered emission in Figure 10b, upon excitation with λ_{ex} = 360−430 nm, which is the absorption region of Au(I) alkynyl based chromophores of compounds **1**−**6**, all the **1**−Yb_2 to **6**−Yb_2 DCM solutions display characteristic Yb(III) centered emission bands with a microsecond range of lifetimes, while the Yb(hfac)$_3$(H_2O)$_2$ DCM solution does not exhibit such a characteristic emission as shown in Figure 10c because no absorption is found for Yb(hfac)$_3$(H_2O)$_2$ in the range 360−430 nm.[27−29] All the above descriptions suggest that effective energy transfer occurs from Au(I) alkynyl chromophores to Yb(III) centers.

$$\frac{1}{\tau_{rad}} = 2303\frac{8\pi cn^2\tilde{\upsilon}_m^2(2J+1)}{N_A(2J'+1)}\int \varepsilon(\tilde{\upsilon})\,d\tilde{\upsilon} \quad (1)$$

$$\Phi = \tau_{obs}/\tau_{rad} \quad (2)$$

The photophysical data of **1**−Yb_2 to **6**−Yb_2 in DCM solutions are presented in Table 3. All the radiative lifetimes

Table 3. Photophysical Data of 1−Yb_2 to 6−Yb_2 in DCM Solutions at 298 K

solution	λ_{abs}^{max}/ nm	λ_{em}^{max}/ nm	$\tilde{\upsilon}_m$/ cm^{-1}	$\int\varepsilon(\tilde{\upsilon})\,d\tilde{\upsilon}$/ $cm^{-2}\,M^{-1}$	τ_{rad}/ μs[a]	τ_{obs}/ μs	Φ_{em}(%)[b]
1-Yb_2	976	979	10373	1204	990	16.1	1.63
2-Yb_2	977	979	10362	1269	941	16.4	1.74
3-Yb_2	977	979	10360	1228	973	16.2	1.66
4-Yb_2	976	979	10359	1246	959	16.2	1.69
5-Yb_2	977	981	10373	1071	1112	16.5	1.48
6-Yb_2	976	980	10364	1198	997	18.1	1.82

[a]Calculated from eq 1. [b]Calculated from eq 2. The **1**−Yb_2 to **6**−Yb_2 solutions were prepared from complexes **1** to **6** and Yb(hfac)$_3$(H_2O)$_2$ according to the corresponding ratio 1:2.

(τ_{rad}) in Table 3 are calculated from eq 1,[55−57] where c, n, N_A, $\tilde{\upsilon}_m$, and $\varepsilon(\tilde{\upsilon})$ are the speed of light in vacuo in cm·s^{-1}, the refractive index of the medium, Avogadro's number, the barycenter of the absorption spectrum of the f−f transition in cm^{-1}, and the absorption coefficient of the f−f transition in M^{-1}·cm^{-1}, respectively. J and J' are the quantum numbers for the ground and excited states, respectively. $\int\varepsilon(\tilde{\upsilon})\,d\tilde{\upsilon}$ is the integrated spectrum of the f−f transition. The intrinsic quantum yields of the Yb(III) emission of **1**−Yb_2 to **6**−Yb_2 solutions at 298 K are in the range 1.48%−1.82%, which are estimated by eq 2, where τ_{obs} is the observed emission lifetime. The intrinsic quantum yields of the Yb(III) emission sensitized by the Au(I)−alkyne antennas, [(tpyC_6H_4C≡CAu)$_2$(μ-PP)] (PP = dppe, dppp, dppb, dpppen, and dpph) and [(bpyC≡CAu)$_2$(μ-pp)] (PP = dppf and dppb),[25,26] and Pt(II)−alkyne antennas, *cis*-[Pt(PP)(C≡CPhtpy)$_2$] (PP = dppm, dppe, and dppp) and [Pt_2(μ-dppm)$_2$(C≡CPhtpy)$_4$], in DCM solutions at 298 K were also reported,[27,28] but it is difficult to compare them with the values here because of the different calculation methods of τ_{rad}, which were taken to be 2 ms in Au(I)−alkyne−Yb(III) and Pt(II)−alkyne−Yb(III) heteronuclear systems on the basis of literature radiative lifetimes.[25−28] The highest intrinsic quantum yield of the Yb(III) emission so far is 9.2%, reported by Hasegawa's group, sensitized by phosphine oxide and fluorinated acetylacetonate ligands and determined in DMSO-d_6 solutions.[57] The intrinsic quantum yields here of **1**−Yb_2 to **6**−Yb_2 are a little lower than that in the Na−Yb heteronuclear complex, 2.6%, sensitized by organic ligand in DCM solution reported by Bünzli's group,[56] but they are still higher than those of most reported Yb(III) complexes, indicating good energy donor ability of complexes **1**−**6**, and this may be attributed to the obvious triplet state emission for the gold(I)−acetylides here at 298 K and lower triplet state energy, and both of the two factors are in favor of energy transfer from Au(I) alkynyl units to the Yb(III) centers.

As shown in Figure 10a and c, complexes **1**−**4** are better energy donors for Yb(IIII) centers than complexes **5** and **6**, and the order of donor ability is **1** ∼ **2** ∼ **3** ∼ **4** > **6** > **5**. Both the nonemissive triplet state at 298 K in DCM solution and the potential intramolecular energy transfer to the ferrocene units for complex **5** are not in favor of energy transfer to the Yb(III) center,[54] and this may be the reason why complex **5** is the worst energy donor.

SUMMARY

In conclusion, a series of dual luminescent 34-membered to 44-membered tetranuclear macrocyclic gold(I) complexes of 5,5′-diethynyl-2,2′-bipyridine ligand have been synthesized. These complexes are suggested to have similar behavior in structures and exhibit similar photophysical properties. All the complexes can behave as energy donors for Yb(III) NIR emission, and the order of donor ability is **1** ∼ **2** ∼ **3** ∼ **4** > **6** > **5**.

ASSOCIATED CONTENT

Supporting Information

Detailed IR data of complexes **1**−**6**, selected bond distances and angles for complexes **1** and **2** (Table S1), absorption spectra titrations between complexes **2**, **3**, **5**, **6**, and Yb(hfac)$_3$(H_2O)$_2$ (Figures S1−S4), luminescent decay profiles (Figures S5−S10), and X-ray crystallographic files in CIF format for the structure determination of **1**·3CH_2Cl_2 and **2**·2C_6H_7N·C_6H_6·2CH_2Cl_2·2H_2O. This material is available free of charge via the Internet at http://pubs.acs.org.

AUTHOR INFORMATION

Corresponding Author

*E-mail: lxl@xznu.edu.cn.

ACKNOWLEDGMENTS

This work was supported financially by NSFC 20801047, the Major Basic Research Project of the Natural Science Foundation of the Jiangsu Higher Education Institutions (11KJA430009), the foundation of Xuzhou Normal University (07XLA07, KY2007039, and XGG2007034), PAPD of Jiangsu Higher Education Institutions, and QingLan Project 08QLT001.

REFERENCES

(1) McArdle, C. P.; Irwin, M. J.; Jennings, M. C.; Puddephatt, R. J. *Angew. Chem., Int. Ed.* **1999**, *38*, 3376.
(2) McArdle, C. P.; Vittal, J. J.; Puddephatt, R. J. *Angew. Chem., Int. Ed.* **2000**, *39*, 3819.
(3) McArdle, C. P.; Jennings, M. C.; Vittal, J. J.; Puddephatt, R. J. *Chem.—Eur. J.* **2001**, *7*, 3572.

(4) Puddephatt, R. J. *Coord. Chem. Rev.* **2001**, *216*−*217*, 313.
(5) McArdle, C. P.; Irwin, M. J.; Jennings, M. C.; Vittal, J. J.; Puddephatt, R. J. *Chem.*—*Eur. J.* **2002**, *8*, 723.
(6) McArdle, C. P.; Van, S.; Jennings, M. C.; Puddephatt, R. J. *J. Am. Chem. Soc.* **2002**, *124*, 3959.
(7) Hunks, W. J.; Lapierre, J.; Jenkins, H. A.; Puddephatt, R. J. *J. Chem. Soc., Dalton Trans.* **2002**, 2885.
(8) Mohr, F.; Eisler, D. J.; McArdle, C. P.; Atieh, K.; Jennings, M. C.; Puddephatt, R. J. *J. Organomet. Chem.* **2003**, *670*, 27.
(9) Mohr, F.; Jennings, M. C.; Puddephatt, R. J. *Eur. J. Inorg. Chem.* **2003**, 217.
(10) Hunks, W. J.; Jennings, M. C.; Puddephatt, R. J. *Z. Naturforsch.* **2004**, *59b*, 1488.
(11) Habermehl, N. C.; Jennings, M. C.; McArdle, C. P.; Mohr, F.; Puddephatt, R. J. *Organometallics* **2005**, *24*, 5004.
(12) Habermehl, N. C.; Eisler, D. J.; Kirby, C. W.; Yue, N. L. S.; Puddephatt, R. J. *Organometallics* **2006**, *25*, 2921.
(13) Habermehl, N. C.; Mohr, F.; Eisler, D. J.; Jennings, M. C.; Puddephatt, R. J. *Can. J. Chem.* **2006**, *84*, 111.
(14) Irwin, M. J.; Rendina, L. M.; Vittal, J. J.; Puddephatt, R. J. *Chem. Commun.* **1996**, 1281.
(15) Tang, H. S.; Zhu, N.; Yam, V. W. W. *Organometallics* **2007**, *26*, 22.
(16) Yam, V. W. W.; Choi, S. W. K.; Cheung, K. K. *Organometallics* **1996**, *15*, 1734.
(17) Che, C. M.; Chao, H. Y.; Miskowski, V. M.; Li, Y.; Cheung, K. K. *J. Am. Chem. Soc.* **2001**, *123*, 4985.
(18) Lu, W.; Xiang, H. F.; Zhu, N.; Che, C. M. *Organometallics* **2002**, *21*, 2343.
(19) Chao, H. Y.; Lu, W.; Li, Y.; Chan, M. C. W.; Che, C. M.; Cheung, K. K.; Zhu, N. *J. Am. Chem. Soc.* **2002**, *124*, 14696.
(20) Lu, W.; Zhu, N.; Che, C. M. *J. Am. Chem. Soc.* **2003**, *125*, 16081.
(21) Lu, X. X.; Li, C. K.; Cheng, E. C. C.; Zhu, N. Y.; Yam, V. W. W. *Inorg. Chem.* **2004**, *43*, 2225.
(22) Li, P.; Ahrens, B.; Bond, A. D.; Davies, J. E.; Koentjoro, O. F.; Raithby, P. R.; Teat, S. J. *Dalton Trans.* **2008**, 1635.
(23) Hunks, W. J.; MacDonald, M. A.; Jennings, M. C.; Puddephatt, P. J. *Organometallics* **2000**, *19*, 5063.
(24) Vicente, J.; Gil-Rubio, J.; Barquero, N.; Jones, P. G.; Bautista, D. *Organometallics* **2008**, *27*, 646.
(25) Li, X. L.; Zhang, K. J.; Li, J. J.; Cheng, X. X.; Chen, Z. N. *Eur. J. Inorg. Chem.* **2010**, 3449.
(26) Xu, H. B.; Zhang, L. Y.; Ni, J.; Chao, H. Y.; Chen, Z. N. *Inorg. Chem.* **2008**, *47*, 10744.
(27) Li, X. L.; Dai, F. R.; Zhang, L. Y.; Zhu, Y. M.; Peng, Q.; Chen, Z. N. *Organometallics* **2007**, *26*, 4483.
(28) Li, X. L.; Shi, L. X.; Zhang, L. Y.; Wen, H. M.; Chen, Z. N. *Inorg. Chem.* **2007**, *46*, 10892.
(29) Xu, H. B.; Zhang, L. Y.; Chen, Z. H.; Shi, L. X.; Chen, Z. N. *Dalton Trans.* **2008**, 4664.
(30) Chen, Z. N.; Fan, Y.; Ni, J. *Dalton Trans.* **2008**, 573.
(31) Xu, H. B.; Shi, L. X.; Ma, E.; Zhang, L. Y.; Wei, Q. H.; Chen, Z. N. *Chem. Commun.* **2006**, 1601.
(32) Xu, H. B.; Zhang, L. Y.; Xie, Z. L.; Ma, E.; Chen, Z. N. *Chem. Commun.* **2007**, 2744.
(33) Ronson, T. K.; Lazarides, T.; Adams, H.; Pope, S. J. A.; Sykes, D.; Faulkner, S.; Coles, S. J.; Hursthouse, M. B.; Clegg, W.; Harrington, R. W.; Ward, M. D. *Chem.*—*Eur. J.* **2006**, *12*, 9299.
(34) Shavaleev, N. M.; Accorsi, G.; Virgili, D.; Bell, Z. R.; Lazarides, T.; Calogero, G.; Armaroli, N.; Ward, M. D. *Inorg. Chem.* **2005**, *44*, 61.
(35) Beer, P. D.; Szemes, F.; Passaniti, P.; Maestri, M. *Inorg. Chem.* **2004**, *43*, 3965.
(36) Shavaleev, N. M.; Moorcraft, L. P.; Pope, S. J. A.; Bell, Z. R.; Faulkner, S.; Ward, M. D. *Chem.*—*Eur. J.* **2003**, *9*, 5283.
(37) Shavaleev, N. M.; Moorcraft, L. P.; Pope, S. J. A.; Bell, Z. R.; Faulkner, S.; Ward, M. D. *Chem. Commun.* **2003**, 1134.
(38) Klink, S. I.; Keizer, H.; van Veggel, F. C. J. M. *Angew. Chem., Int. Ed.* **2000**, *39*, 4319.
(39) Grosshenny, V.; Romero, F. M.; Ziessel, R. *J. Org. Chem.* **1997**, *62*, 1491.
(40) Hasegawa, Y.; Kimura, Y.; Murakoshi, K.; Wada, Y.; Kim, J. H.; Nakashima, N.; Yamanaka, T.; Yanagida, S. *J. Phys. Chem.* **1996**, *100*, 10201.
(41) Rigaku. *CrystalClear*; Rigaku Corporation: Tokyo, Japan, 2005.
(42) Rigaku. *CrystalStructure*; Rigaku Corporation: Tokyo, Japan, 2007.
(43) Bruker. *SAINT-Plus*; Bruker AXS Inc.; Madison, WI, USA, 2003.
(44) Sheldrick, G. M. *SHELXL-97, Program for the Refinement of Crystal Structures*; University of Göttingen: Göttingen, Germany, 1997.
(45) Irwin, M. J.; Jia, G.; Payne, N. C.; Puddephatt, R. J. *Organometallics* **1996**, *15*, 51.
(46) Irwin, M. J.; Vittal, J. J.; Yap, G. P. A.; Puddephatt, R. J. *J. Am. Chem. Soc.* **1996**, *118*, 13101.
(47) Brandys, M. C.; Jennings, M. C.; Puddephatt, R. J. *J. Chem. Soc., Dalton Trans.* **2000**, 4601.
(48) Wong, K. M. C.; Hung, L. L.; Lam, W. H.; Zhu, N.; Yam, V. W. W. *J. Am. Chem. Soc.* **2007**, *129*, 4350.
(49) Hogarth, G.; Álvarez-Falcón, G. M. *Inorg. Chim. Acta* **2005**, *358*, 1386.
(50) MacDonald, M. A.; Puddephatt, R. J. *Organometallics* **2000**, *19*, 2194.
(51) Dietrich-Buchecker, C. O.; Sauvage, J. P. *Chem. Commun.* **1999**, 615.
(52) Ibukuro, F.; Fujita, M.; Yamaguchi, K.; Sauvage, J. P. *J. Am. Chem. Soc.* **1999**, *121*, 11014.
(53) Deák, A.; Tunyogi, T.; Tárkányi, G.; Király, P.; Pálinkás, G. *CrystEngComm* **2007**, *9*, 640.
(54) Armaroli, N.; Accorsi, G.; Bergamini, G.; Ceroni, P.; Holler, M.; Moudam, O.; Duhayon, C.; Delavaux-Nicot, B.; Nierengarten, J. *Inorg. Chim. Acta* **2007**, *360*, 1032.
(55) Werts, M. H. V.; Jukes, R. T. F.; Verhoeven, J. W. *Phys. Chem. Chem. Phys.* **2002**, *4*, 1542.
(56) Shavaleev, N. M.; Scopelliti, P.; Gumy, F.; Bünzli, J. C. G. *Inorg. Chem.* **2009**, *48*, 7937.
(57) Kishhimoto, S. I.; Nakagawa, T.; Kawai, T.; Hasegawa, Y. *Bull. Chem. Soc. Jpn.* **2011**, *84* (2), 148.